

## RELATION BETWEEN COAL STRUCTURE AND THERMAL DECOMPOSITION PRODUCTS

P. R. Solomon

United Technologies Research Center  
East Hartford, CT 06108

### INTRODUCTION

In a recent study, the thermal decomposition of 13 coals was examined in over 600 vacuum devolatilization experiments (1). The results for all 13 coals were successfully simulated in a model which assumes the evolution of tar "monomers" from the coal "polymer" and the parallel evolution of smaller molecular species produced by further cracking of the molecular structure (2,3). The evolution of each species is characterized by rate constants which do not vary with coal rank. The differences between coals are due to differences in the mix of sources in the coal for the evolved species. The sources were tentatively related to the functional group concentrations in the coal.

This paper reports a study to verify the relationship between functional group distribution and thermal decomposition behavior. A Fourier Transform Infrared Spectrometer (FTIR) has been employed to obtain quantitative infrared spectra of the coals, chars and tars produced in the devolatilization experiments. The spectra have been deconvoluted using a computerized spectral synthesis routine to obtain functional group distributions, which are compared to the model parameters.

### MODEL

The thermal decomposition model is illustrated in Fig. 1. The initial coal composition (Fig. 1a) is described by the fraction  $Y_i^0$  of each functional group present ( $\sum_i Y_i^0 = 1$ ) and the fraction of coal  $X^0$  which is potentially tar forming. During decomposition each component may evolve as an independent species into the gas or may evolve with the tar. The evolution of a component into the tar is described by the diminishing of the  $X$  dimension and into the gas by the diminishing of the  $Y_i$  dimensions according to

$$X = X^0 \exp(-k_X t) \quad \text{and} \quad Y_i = Y_i^0 \exp(-k_i t)$$

where  $k_i$  and  $k_X$  are rate constants given in Table I.

According to this model the tar contains a mix of functional groups similar to that in the parent coal. This concept is based on the strong similarity between vacuum devolatilized tar and the parent coal observed in chemical composition (1,2,3), infrared spectra (1,3,4,5), and nmr spectra (1,3). The similarity of the infrared spectra is illustrated in Fig. 2 for four coals. The resemblance of the tar and parent coal suggests that the tar consists of "monomers" released from the coal "polymer". The major difference observed in the ir spectra between tar and parent coal is the higher quantity of aliphatic\*  $\text{CH}_2$  and  $\text{CH}_3$ . This is presumably

\* No attempt has been made in this paper to distinguish between aliphatic and alicyclic CH.

because the monomers abstract hydrogen to stabilize the free radical sites produced when the monomer was freed. Similar arguments were given for pyrolysis of model compounds by Wolfs, van Krevelen and Waterman (6).

TABLE I KINETIC CONSTANTS FOR LIGNITE AND BITUMINOUS COALS (2)

Functional Group	Kinetic Rates
carboxyl	$k_1 = 6 \exp(-4000/T) \text{ sec}^{-1}$
hydroxyl	$k_2 = 15 \exp(-4950/T)$
ether	$k_3 = 890 \exp(-12000/T)$
aliphatic	$k_4 = 4200 \exp(-9000/T)$
aromatic H	$k_5 = 3600 \exp(-12700/T)$
aromatic C	$k_6 = 0$
tar	$k_X = 750 \exp(-8000/T)$

Figure 1b illustrates the initial stage of thermal decomposition during which the volatile components  $\text{H}_2\text{O}$  and  $\text{CO}_2$  evolve from the hydroxyl and carboxyl groups respectively along with aliphatics and tar. At a later stage (Fig. 1c)  $\text{CO}$  and  $\text{H}_2$  are evolved from the ether and aromatic H.

To simulate the abstraction of H by the tar, the aliphatic fraction in the tar is assumed to be retained together with some additional aliphatic material which may be added directly or may contribute its hydrogen. When hydrogen from the aliphatic material is contributed, its associated carbons remain with the aromatic carbon fraction which eventually forms the char (Fig. 1d).

#### INFRARED SPECTRA

Infrared Spectra of coals, tars and chars were obtained on a Nicolet FTIR. KBr pellets of coals and chars were prepared by mixing 1 mg of dry, finely ground (20 min in a "Wig-L-Bug") sample with 300 mg of KBr. Thirteen mm diameter pellets were pressed in an evacuated die under 20,000 lbs pressure for one minute and dried at  $110^\circ\text{C}$  overnight to remove water. Since the heating process destroyed similarly prepared tar pellets, the water correction was obtained by subtracting the spectrum of a blank disk prepared under the same conditions. The  $\text{H}_2\text{O}$  corrected spectra matched those from samples prepared by allowing the tar produced in thermal decomposition to fall directly onto a water free blank KBr disk.

The FTIR obtains spectra in digital form and corrections for particle scattering, mineral content and water may be easily made. A typical correction sequence is illustrated in Fig. 3. The lower curve is the uncorrected spectrum of a dried coal. It has a slope due to particle scattering and peaks from the mineral components near  $1000$  and  $450 \text{ cm}^{-1}$ . In the middle figure a straight line scattering spectrum has been subtracted. In the top the spectrum for a mixture of kaolin and illite has been subtracted (7) and the spectrum scaled to give the absorbance for 1 mg of coal dmmf.

Much previous work has been done to identify the functional groups responsible for the observed peaks. Extensive references may be found in Lowry (8) and van Krevelen (9). To get a quantitative measure of the functional group concentrations, a curve analysis program (CAP) available in the Nicolet library was used to synthesize the ir spectra. The synthesis is accomplished by adding 26 absorption peaks

with Gaussian shapes and variable position, width, and height as shown in Fig. 4. The peaks are separated according to the identified functional group. It has been determined that all the coals, chars, and tars which were studied could be synthesized by varying only the magnitudes of a set of Gaussians whose widths and positions were held constant. These samples could therefore be analyzed in terms of a fixed mix of functional groups.

Peak O at  $1600\text{ cm}^{-1}$  has been included with the hydroxyl group. The identity of this peak has caused much speculation in the literature (8,9). Fujii et al. (10), showed that the intensity of the  $1600\text{ cm}^{-1}$  peak varied linearly with oxygen content in the coal. The present study narrows the correlation still further. Figure 5 shows a linear relation between the intensity of the O peak at  $1600\text{ cm}^{-1}$  and the hydroxyl content measured by peaks L, M, N and Q. The correlation includes chars which have a high oxygen content in ether groups but very low hydroxyl so that the correlation with total oxygen would no longer hold. It has, therefore, been concluded that the sharp line at  $1600\text{ cm}^{-1}$  is caused mainly by hydroxyl oxygen probably in the form of phenols.

The calibration of the aliphatic peaks near  $2900\text{ cm}^{-1}$  (lines A-E) and the aromatic peaks near  $800\text{ cm}^{-1}$  (lines I-K) is shown in Fig. 6. The objective is to determine the values of the constants a and b, which relate peak areas to the corresponding hydrogen concentration, i.e.,

$$H_{\text{ali}} = a A_{\text{ABCDE}} \quad \text{and} \quad H_{\text{aro}} = b A_{\text{IJK}}$$

where  $A_{\text{ABCDE}}$  is the area under the aliphatic peaks A-E,  $A_{\text{IJK}}$  is the area under the aromatic peaks I-K, and  $H_{\text{ali}}$  and  $H_{\text{ar}}$  the aliphatic (or alicyclic) and aromatic hydrogen concentrations, respectively. The equation for total hydrogen concentration  $H_{\text{total}} = H_{\text{ali}} + H_{\text{ar}} + H_{\text{hydroxyl}}$  may be combined with the above equations to yield

$$a \left[ \frac{A_{\text{ABCDE}}}{H_{\text{total}} - H_{\text{hydroxyl}}} \right] = 1 - b \left[ \frac{A_{\text{IJK}}}{H_{\text{total}} - H_{\text{hydroxyl}}} \right]$$

where  $H_{\text{hydroxyl}}$  is the hydrogen content in hydroxyl groups obtained from

$$H_{\text{hydroxyl}} = c A_{\text{LMNQ}}$$

where c has been determined using the relation between hydroxyl content and specific extinction coefficient at  $3450\text{ cm}^{-1}$  derived by Ōsawa and Shih (11).

The hydrogen distribution computed using the determined values of  $a = .075$  and  $b = .071$  are shown in Table II. In the present investigation it was felt that the determination of peak areas rather than peak intensities would be more accurate method for determining quantitative functional group concentrations. For comparison to other infrared investigations more useful relations are

$$H_{\text{ali}} = 11.5 \times D_{\text{ali}} A/M \% \quad \text{and} \quad H_{\text{aro}} = 19.2 \times D_{\text{aro}} A/M \%$$

where A is the area of the pellet in  $\text{cm}^2$ , m the sample weight in mg,  $D_{\text{ali}}$  is the optical density of the peak at  $2920^{-1}$  and  $D_{\text{aro}}$  is the average optical density of the I, J, and K peaks near  $800\text{ cm}^{-1}$ .

TABLE II HYDROGEN DISTRIBUTION IN COALS (dmf)

COAL	PLOTING SYMBOL	C	H	O	From IR			
					H <sub>aro</sub>	H <sub>ali</sub>	H <sub>hydr</sub>	H <sub>aro</sub> /H <sub>ali</sub>
PSOC 268	M	86.2	5.24	6.13	2.2	2.8	.28	.79
PSOC 124	B	84.8	7.17	6.35	1.6	6.0	.42	.27
PSOC 170	G	81.8	5.37	9.12	1.8	3.2	.31	.56
PSOC 103	A	82.9	5.11	10.04	2.0	2.4	.36	.83
Bu Mi 40660	Z	79.9	5.32	11.74	2.0	3.1	.42	.65
PSOC 330	V	80.4	5.09	12.21	1.9	2.8	.42	.68
PSOC 212	J	76.2	4.81	16.81	1.5	2.5	.58	.60
PSOC 308	T	74.0	5.11	18.14	1.7	3.0	.58	.57
Montana	4	65.2	3.60	29.44	1.1	1.7	.71	.65
Lignite								

The aromatic hydrogen values are in agreement with those determined by van Krevelen (8) and by Mazumdar, et al. (11), from pyrolysis measurements but are larger (by about a factor of 2) than those determined by Brown (12) using infrared techniques. Brown measured the ratio of extinction coefficients at 3030 cm<sup>-1</sup> (line H) and 2920 cm<sup>-1</sup> (line D) and used an assumed value of 2 (this value has been open to question) for the ratio of absorption strength for aliphatic and aromatic C-H bonds. The ratio of extinction coefficients determined in the present study are in reasonable agreement with those determined by Brown thus the absorption strength ratio must be approximately 4 to produce the measured values of H<sub>aro</sub>/H<sub>ali</sub>.

#### THERMAL DECOMPOSITION

The progress of thermal decomposition is illustrated by the series of spectra for chars in Fig. 7. The chars were produced by devolatilizing coal PSOC 212 for 80 sec at the indicated temperature. The results are similar to those observed by Brown (13) and Oelert (14). The rapid disappearance of the aliphatic and hydroxyl peaks is apparent. The temperature and time dependence of the decrease in these groups is in agreement with the kinetic constants of Table I obtained from analysis of the gas components and elemental composition of the char and tar in thermal decomposition. The aromatic peaks remain to high temperature and the ether peaks are observed to increase in intensity possibly from the creation of new ether linkages by



For high temperature chars whose carbon content exceeds 92 percent a broad absorption begins to dominate the spectrum. This is similar to the effect observed in high rank coals (above 92% C) which has been attributed to electronic absorption (8,9).

Figure 8 shows the quantitative determination of the hydrogen functional group distribution for the chars in Fig. 7. Figure 9 shows the measured hydrogen content and model prediction. The agreement is good. Comparison of Figs. 8 and 9 clearly shows how the low temperature loss of aliphatic material and tar and the retention

of aromatic hydrogen produced the observed shape for the curve of total hydrogen content vs. temperature. The distribution of other products of thermal decomposition for the same coal is shown in Figs. 10 and 11.

The thermal decomposition model was developed using model parameters derived from the decomposition experiments (1,2,3). The observed relationship between the products and the functional group compositions determined from ir measurements indicates that several of these model parameters may be obtained directly from the ir spectra. A comparison of parameters determined from the thermal decomposition experiments with those determined from the ir measurements is made in Fig. 12. Additional parameters may also be determined in the same way.

### CONCLUSIONS

The results of the present investigation have yielded the following conclusions:

1. FTIR provides a convenient tool for obtaining quantitative infrared spectra of coals, chars and tars on a dry mineral matter free basis.
2. The spectra of all the coals, chars and tars studied could be deconvoluted by varying the magnitudes of a set of 26 Gaussians whose width and position were held constant. This provides a good way for determining magnitudes of individual peaks.
3. Correlation of the magnitudes of the  $1600\text{ cm}^{-1}$  peak with the hydroxyl content of a variety of coals, tars and chars indicates that hydroxyl, probably in the form of phenols, contributes strongly to this peak.
4. A regression analysis applied to a series of coals, chars and tars with widely differing ratios of aliphatic to aromatic hydrogen has been used to calibrate the aliphatic and aromatic C-H absorption intensities.
5. The values of aromatic hydrogen for coals derived from the infrared analysis are in reasonable agreement with those of van Krevelen (8) and Mazumdar (11) but are roughly a factor of 2 larger than those derived by Brown (12).
6. Infrared spectra of a series of coals and tars demonstrate the very close similarity of tars to their parent coals providing further evidence that the tar consists of hydrogen stabilized "monomers" derived from decomposition of the coal "polymer".
7. The variation of functional group concentrations in the products of thermal decomposition is in good agreement with the predictions of a detailed thermal decomposition model (1,2,3).
8. Most of the coal parameters used in the thermal decomposition model may be obtained directly from an infrared, ultimate and proximate analysis of the coal allowing prediction of thermal decomposition behavior from a general set of kinetic constants applicable to lignite and bituminous coals.

### ACKNOWLEDGEMENT

The author wishes to acknowledge the able technical assistance of David Santos and Gerald Wagner and helpful discussions with Med Colket and Daniel Seery. The thermal decomposition studies upon which this work was based was supported in part by Grant #AER75-17247 from the National Science Foundation under the technical supervision of the Department of Energy.

# REFERENCES

1. Solomon, P. R., "The Evolution of Pollutants During the Rapid Devolatilization of Coal," Report NSF/RA-770422, NTIS #PB278496/AS.
2. Solomon, P. R., and Colket, M. B.: Seventeenth Symposium (International) on Combustion, the Combustion Institute (to be published).
3. Solomon, P. R., and Colket, M. B.: Fuel, to be published.
4. Orning, A. A., Greifer, B.: Fuel 35, 381 (1956).
5. Brown, J. K., Dryden, I. G. C., Dunevein, D. H., Joy, W. K., and Pankhurst, K. S.: J. Inst. Fuels 31, 259 (1958).
6. Wolfs, P. M. J., van Krevelen, D. W. and Waterman, H. I.: Fuel 39 25, (1960).
7. Painter, P. C., Coleman, M. M., Jenkins, R. G., and Walker, P. L., Jr.: Fuel 57 124 (1978).
8. Lowry, H. H.: Chemistry of Coal Utilization (Supplementary Volume), Wiley, NY (1963).
9. van Krevelen, D. W., and Schuyer, J.: Coal Science, Elsevier, Amsterdam (1957).
10. Fujii, S., Ōsawa, Y., and Sugimura, H.: Fuel 49 68 (1970).
11. Ōsawa, Y., and Shih, J. W.: Fuel 50 53 (1971).
12. Brown, J. K.: J. Chem. Soc. 744 (1955).
13. Brown, J. K.: J. Chem. Soc. 752 (1955).
14. Oelert, H. H.: Fuel 47 433 (1968).

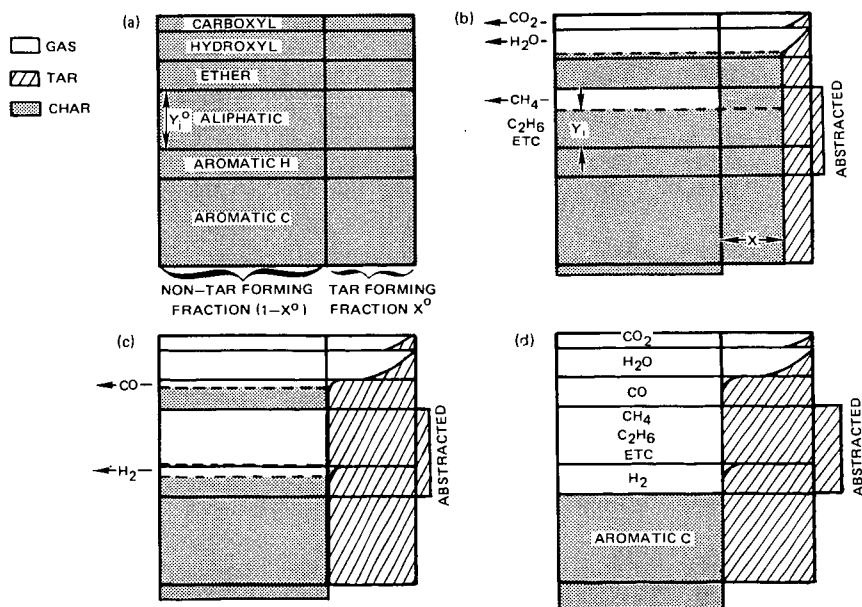


Figure 1 Progress of Thermal Decomposition a) Functional Group Composition of Coal  
b) Initial Stage of Decomposition c) Later Stage of Decomposition  
d) Completion of Decomposition

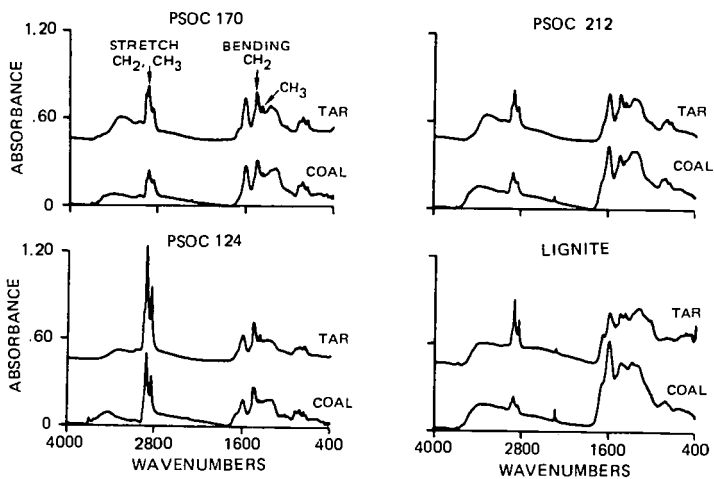


Figure 2. Infrared Spectra of Coals and Tars

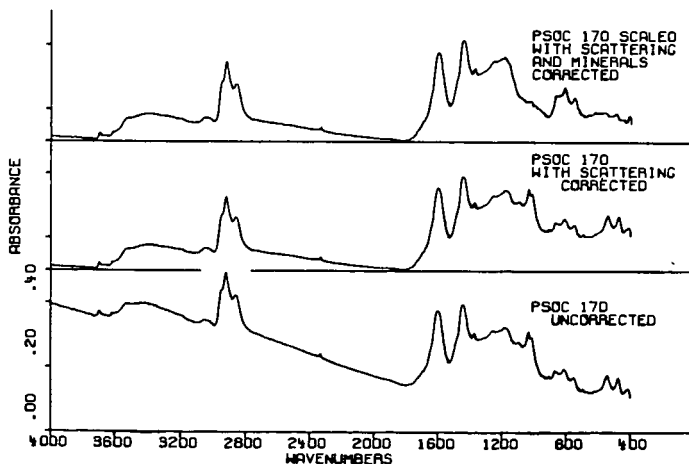


Figure 3. Correction of Coal Spectrum for Scattering and Minerals

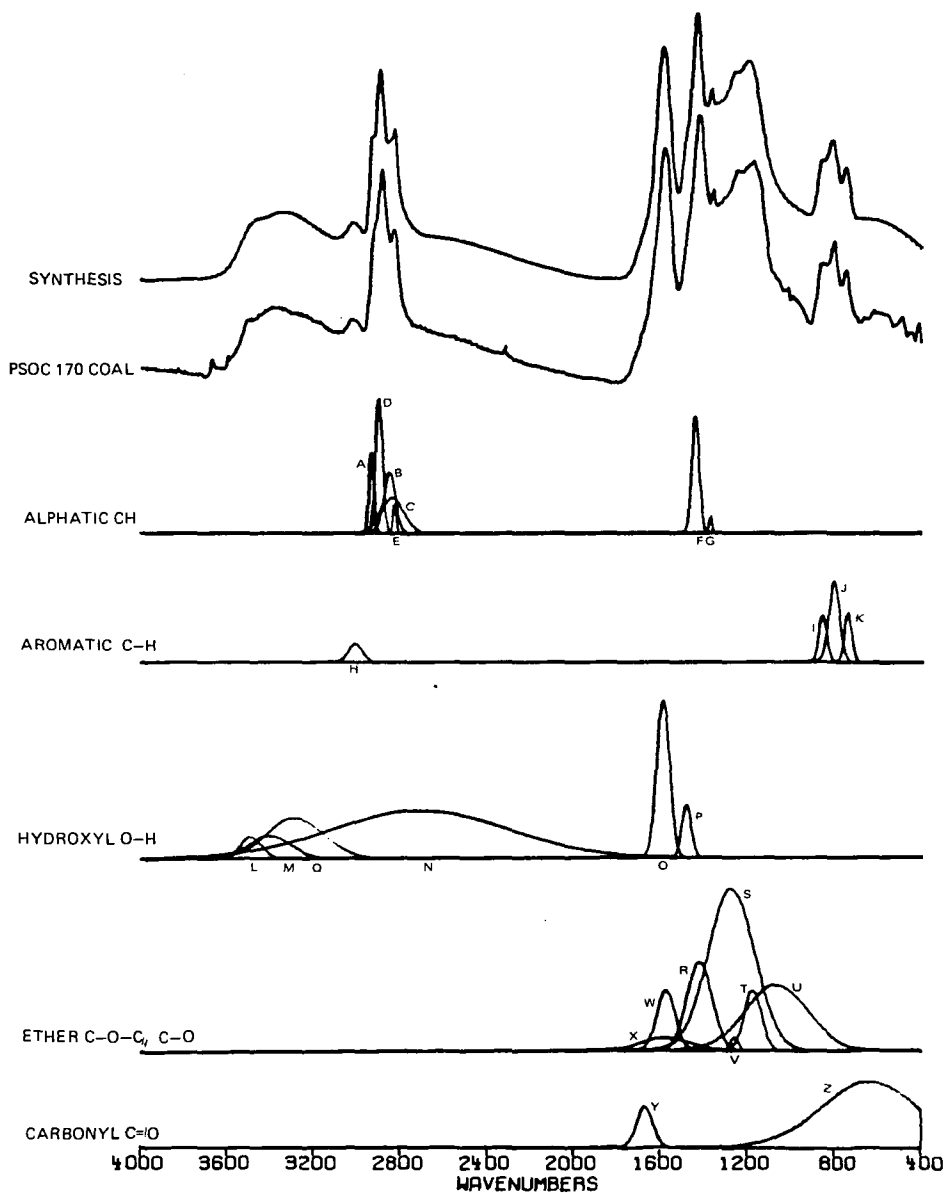


Figure 4. Synthesis of Infrared Spectrum

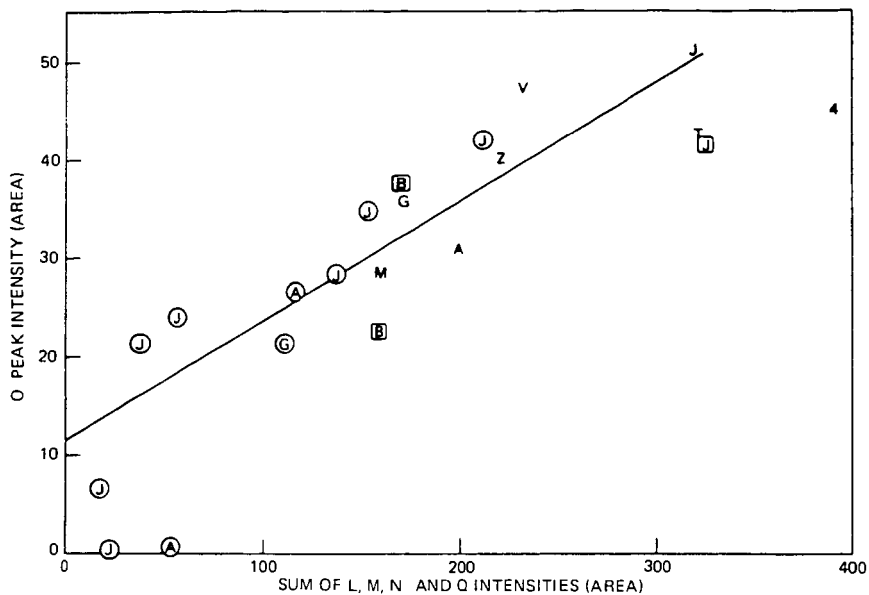


Figure 5. Correlation of  $1600\text{ cm}^{-1}$  Absorption with OH Absorption Intensity. Letters Designate Coals; See Table II.  $\circ$  Chars  $\square$  Tars

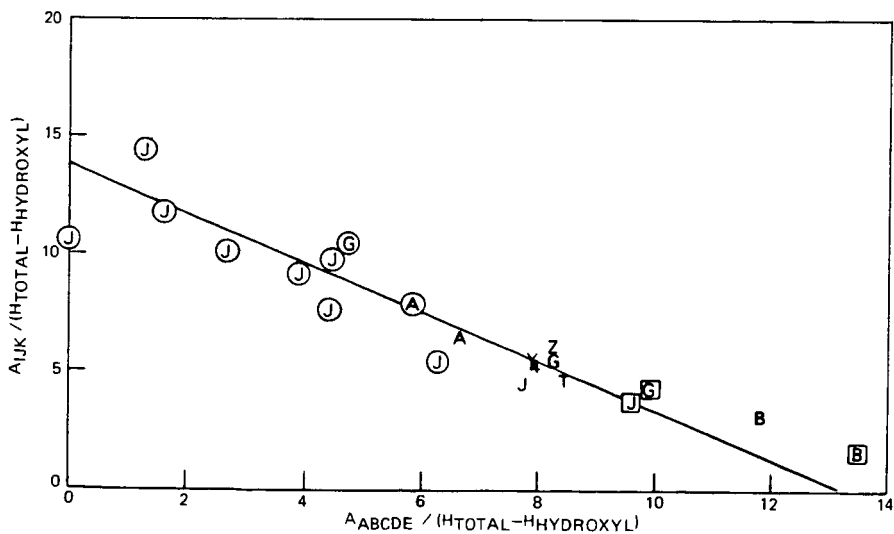


Figure 6. Calibration of Aromatic and Aliphatic Absorption Peaks. Letters Designate Coals; See Table II.  $\circ$  Chars  $\square$  Tars

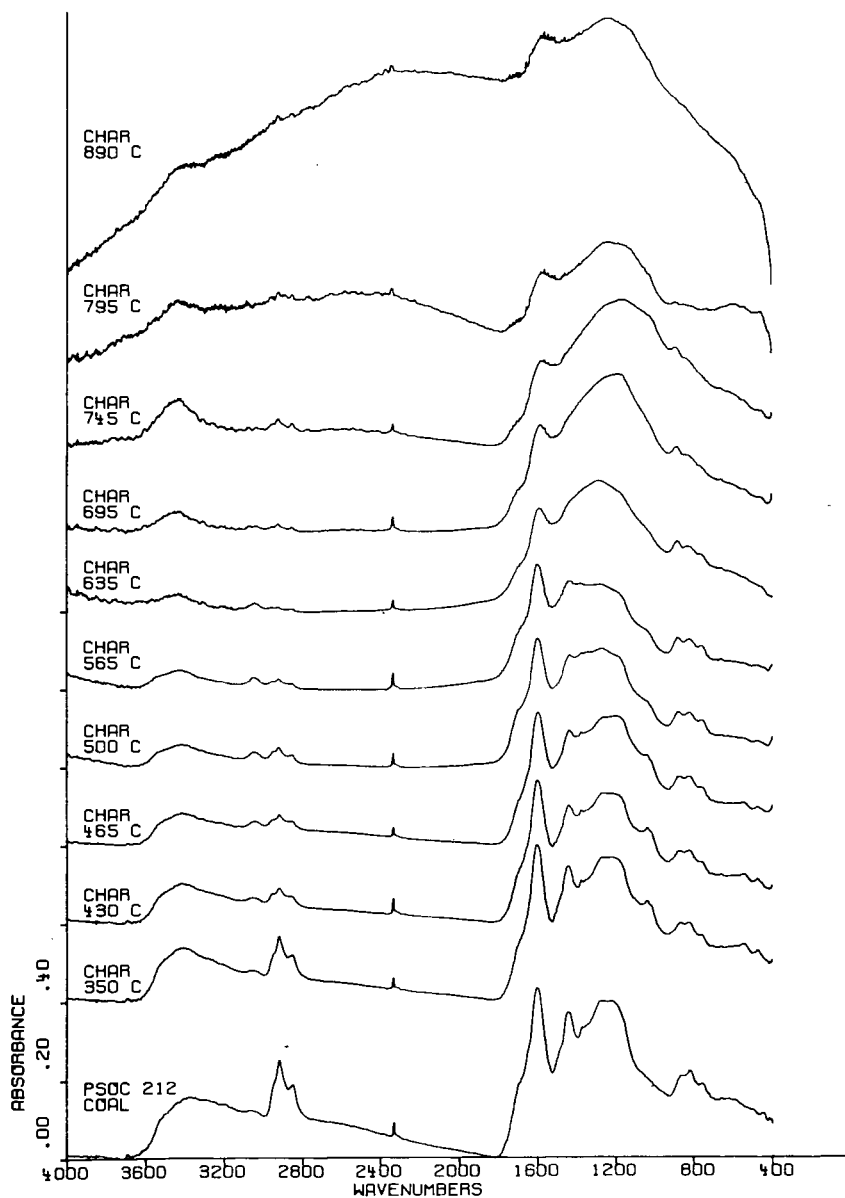


Figure 7. Spectra of Chars

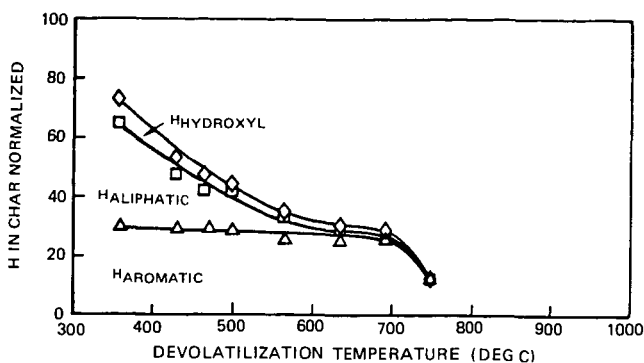


Figure 8. Hydrogen Distribution in Char from Infrared Analysis – The Hydrogen in the Char is Normalized by the Amount of Hydrogen in the Starting Coal Sample

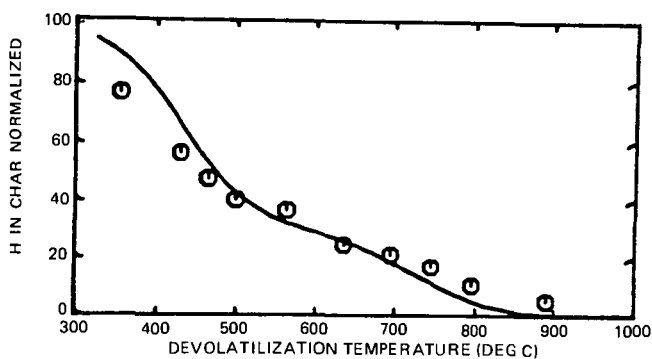


Figure 9. Hydrogen in Char—Experiment and Theory – The Hydrogen in the Char is Normalized by the Amount of Hydrogen in the Starting Coal Sample.

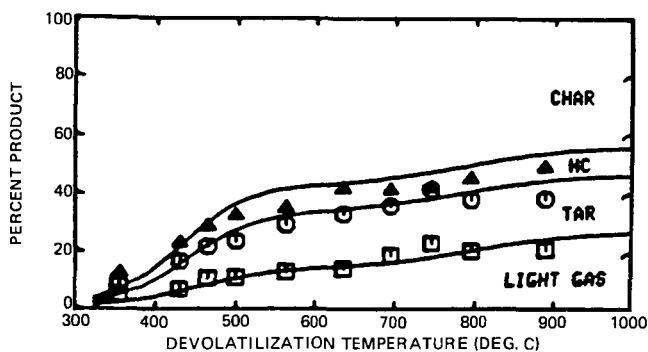


Figure 10. Products of Thermal Decomposition – Experiment and Theory

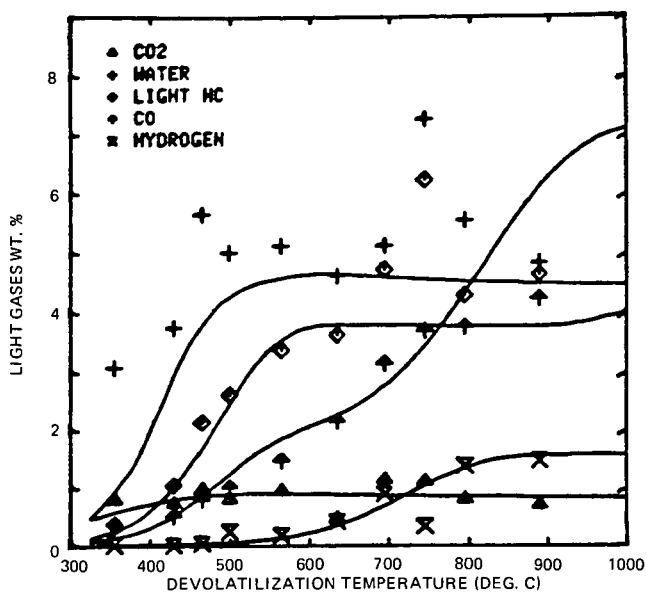


Figure 11. Products of Thermal Decomposition – Experiment and Theory

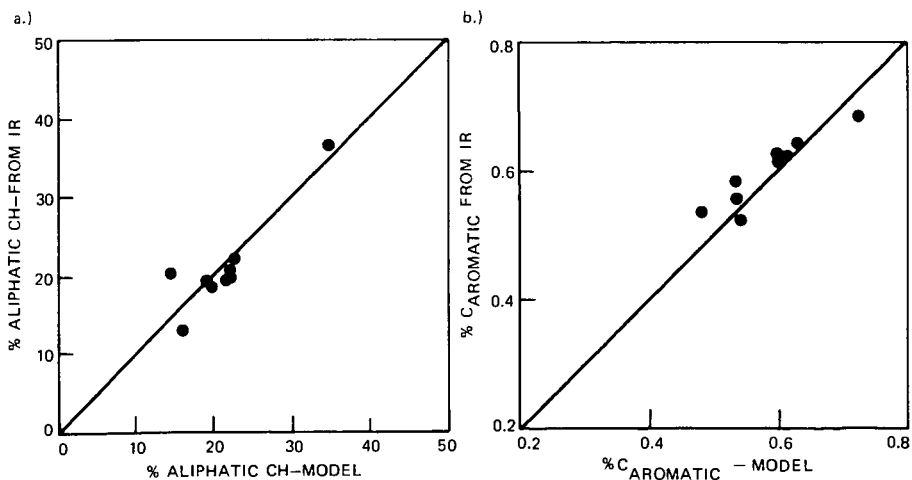


Figure 12. Comparison of Model Parameters with IR Intensity